View metadata, citation and similar papers at core.ac.uk
brought to you by CORE
provided by Texas A&M University

PHYSICAL REVIEW C **86**, 011304(R) (2012)

# Two-proton decay of $^{12}$O and its isobaric analog state in $^{12}$N

M. F. Jager, R. J. Charity, J. M. Elson, J. Manfredi, M. H. Mahzoon, and L. G. Sobotka
*Departments of Chemistry and Physics, Washington University, St. Louis, Missouri 63130, USA*

M. McCleskey, R. G. Pizzone,* B. T. Roeder, A. Spiridon, E. Simmons, and L. Trache
*Cyclotron Institute, Texas A&M University, College Station, Texas 77843, USA*

M. Kurokawa
*RIKEN Nishina Center, Wako, Saitama 351-0198, Japan*

(Received 1 May 2012; published 26 July 2012; corrected 8 November 2012)

Following neutron knockout from an $^{13}$O beam, $^{12}$O fragments were created and the three decay products following two-proton decay were detected. A new ground-state mass was determined by the invariant mass method implying a decay kinetic energy of 1.638(24) MeV, and the width was found to be less than 72 keV. The latter is inconsistent with previous measurements with lower experimental resolutions but consistent with theoretical estimates. The isobaric analog of $^{12}$O in $^{12}$N was produced from proton knockout reactions with the same beam and decayed by two-proton emission to the isobaric analog state in $^{10}$B with a decay kinetic energy of 1.165(29) MeV. It represents only the second case of an analog state where two-proton decay is the only isospin- and energy-conserving particle decay mode. With our measurements of the mass excesses of $^{12}$O and its analog, the quadratic form of the isobaric multiplet mass equation was found to fit the $A = 12$ quintet and any deviations are less than the magnitude found for the $A = 8$ quintet and $A = 7$ and 9 quartets.

DOI: 10.1103/PhysRevC.86.011304 PACS number(s): 23.50.+z, 21.10.Dr, 25.60.−t, 27.20.+n

Although the ground state of $^{12}$O was shown to undergo two-proton decay more than 15 years ago [1], a full description of the decay has not been obtained. Based on tabulated masses (AME2011) [2], its decay kinetic energy is $E_T = 1.771$ (18) MeV. The distribution of the opening angle between the two protons in the $^{12}$O frame was found to be inconsistent with the simplistic diproton decay scenario with a 7% upper limit for this decay branch [1]. However, consistency between the two-proton energy difference and opening angles was found for a sequential two-proton decay scenario through the $^{11}$N $J^\pi = 1/2^+$ ground state [3]. As shown in Fig. 1(a), $^{12}$O is not a Goldansky-type two-proton emitter where no intermediate state is energetically accessible [4]. The location of $^{11}$N$_{\text{g.s.}}$ was not known at the time of the original experiment [1] and even now there is some uncertainty as to its exact location and width [5–9]. Reported widths range from 240(240) keV to 1.44(20) MeV. For the larger values, the lifetime of $^{11}$N$_{\text{g.s.}}$ is too short for a real separation between the two possible decay steps. This would put $^{12}$O decay in a similar category as $^{6}$Be and $^{8}$C two-proton decays where the decay energy is also comparable to the width of the intermediate state and thus cannot be understood as a sequential-decay process [10,11].

The width of $^{12}$O$_{\text{g.s.}}$ itself is also not well understood. The experimental values of 400(250) keV [12], 578(205) keV [1], and 600(500) keV [13] are all large and required significant corrections due to the detector response. However, Sherr and Fortune [14] quote an unpublished value of less than 100 keV from double-charge-exchange studies using $\pi^+$ ions [15]. These experimental values can be compared to theoretical estimates of ∼100 keV or less from sequential and three-body decay calculations [14,16,17]. A new study with better experimental resolution is required to resolve this issue.

Some aspects of isospin symmetry can be tested by the isobaric multiplet mass equation (IMME) [18]. To the extent that isospin $T$ is a good quantum number, the energies of the multiplet should be independent of $T_Z$ in the absence of Coulomb forces. If two-body forces are responsible for charge-dependent effects, Wigner found the mass excesses can be described by a quadratic dependence:

$$\Delta M(T, T_Z) = a + b\,T_Z + c\,T_Z^2. \quad (1)$$

Typically cubic and quartic terms ($d\,T_Z^3 + e\,T_Z^4$) are added to the IMME to provide a measure of any deviation from the quadratic form associated with isospin symmetry. The largest deviations as measured by the magnitudes of the $d$ and $e$ coefficients have been found for $A = 7$, 8, and 9 [18–20]. The $A = 12$ quintet is of interest, being the next quintet above $A = 8$ that one can consider investigating. However, it has one member missing, i.e., the isobaric analog state (IAS) of $^{12}$O$_{\text{g.s.}}$ in $^{12}$N.

The ground state of $^{8}$C was found to undergo two steps of two-proton decay forming the $4p + \alpha$ exit channel [11]. The isobaric analog of this state in $^{8}$B was also found to undergo two-proton decay to the isobaric analog state in $^{6}$Li. Based on a rough estimate of the mass of the IAS in $^{12}$N, obtained by fitting the known members with the IMME, we also expect this state to have a significant two-proton decay branch, this time to the IAS in $^{10}$B. This is illustrated in Fig. 1(b) which shows that the isospin-conserving single-nucleon decay modes $n + {}^{11}$N ($T = 3/2$) and $p + {}^{11}$C ($T = 3/2$) are energetically forbidden, making two-proton decay the only isospin- *and* energy-conserving decay mode. Sequential two-proton decay

*Permanent address: INFN, Laboratori Nazionali del Sud, Catania, Italy.

 ©2012 American Physical Society

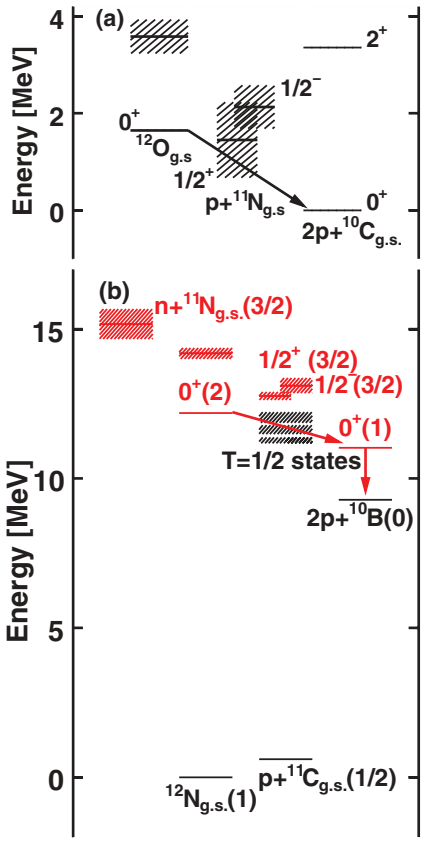


FIG. 1. (Color online) Level diagrams showing the states of interest in the two-proton decays of (a) $^{12}$O levels and (b) their isobaric analogs in $^{12}$N. In (b), not all states are shown; the intermediate states that conserve isospin have their isospin indicated in the parenthesis (red). Also for $^{11}$C, the possible isospin violating $T = 1/2$ intermediate states are indicated. The $^{11}$N levels in both (a) and (b) are not well determined and the results from Ref. [6] were used here.

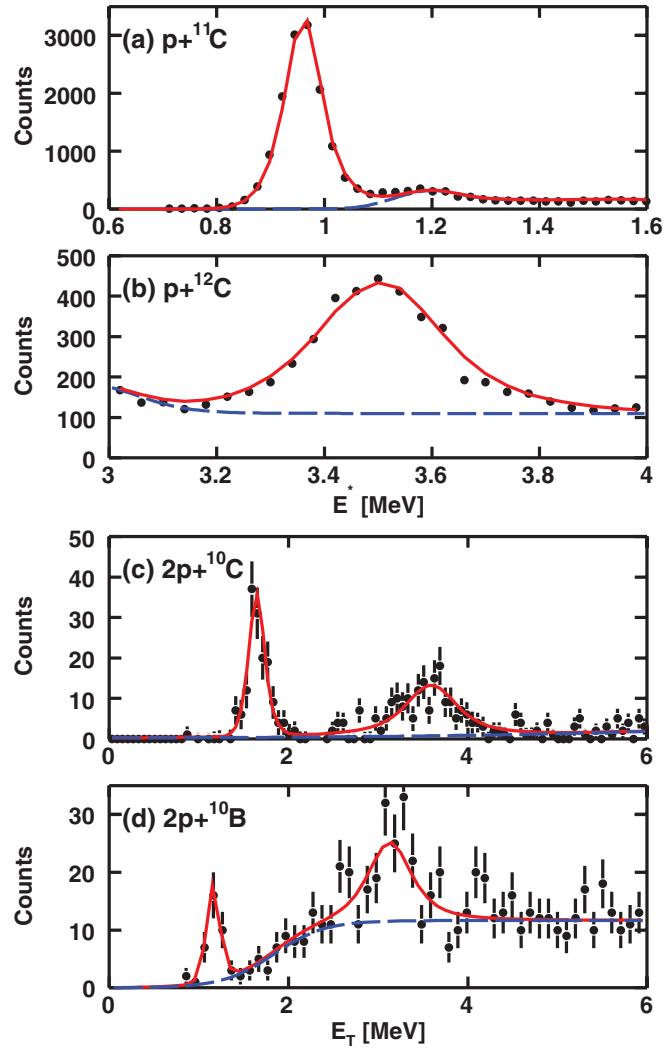


FIG. 2. (Color online) Excitation-energy spectra of calibration peaks for (a) the 960-keV, $J^\pi = 2^+$ state in $^{12}$N and (b) the 3.502 - MeV, $J^\pi = 3/2^-$ level in $^{13}$N. The solid curves show the results of Monte Carlo simulations of the peak shapes incorporating the detector response and the known level properties. The dashed curves indicate an estimation of the background under these peaks. Spectra of total kinetic energy released in the two-proton decay of (c) $^{12}$O and (d) its analog in $^{12}$N reconstructed from detected $2p + ^{10}$C and $2p + ^{10}$B events. The solid curves show peak fits to these data, with the dashed curves indicating the fitted background.

through some relatively narrow ($\Gamma = 200$–$360$ keV) $T = 1/2$ $^{11}$C states (Fig. 1) is energetically allowed, but isospin forbidden.

In this work we report on an experiment with an $^{13}$O secondary beam, using neutron and proton knockout reactions to populate $^{12}$O$_{g.s.}$ and its IAS in $^{12}$N. The two-proton decays of these states were detected and used to deduce the masses and upper limits for the decay widths of these states. At the Texas A&M University cyclotron facility, a primary beam of $E/A = 38$ MeV $^{14}$N of intensity 80 pnA was extracted from the K500 cyclotron. This beam impinged on a hydrogen gas cell held at a pressure of 2.5 atm at liquid nitrogen temperature. A secondary beam of 2000–4000 s$^{-1}$ $E/A = 30.3$ MeV $^{13}$O, separated from the other reaction products using the MARS spectrometer [21,22], impinged on a 45.6 mg/cm$^2$ target of $^9$Be. This secondary beam has a momentum resolution of $\Delta p/p = \pm 0.6\%$ and a purity of 83% with $^{10}$C being the largest contaminant (10%).

The beam and target properties are very similar to those of the original $^{12}$O two-proton experiment of Kryger *et al.* [1]. The biggest improvement in the present study is the use of a large-area double-sided Si strip detector to obtain improved angular resolution for all the detected decay products. The beam and reaction products were incident on a 10 cm $\times$ 10 cm $\times$ 300 $\mu$m Si $\Delta E$ detector with 128 strips on both the front and back sides. The particles of interest pass through this Si detector, which is located 18 cm from the target, and are stopped by a 32-element array of CsI(Tl) scintillator $E$ detectors located immediately behind it. These CsI(Tl) detectors are arranged in a $6 \times 6$ array with the corner locations vacant. Energy calibration of the Si strips was obtained from $^{228}$Th and $^{241}$Am $\alpha$-particle sources, and cocktail beams of various energies were used to calibrate the particle-dependent light output of the CsI(Tl) detectors. These include $p$, $^{10}$B, $^{10}$C, and $^{12}$C beams.

To have confidence in the extracted masses and widths, it is useful to compare them to well-known "calibrations" states. Figures 2(a) and 2(b) show the $^{12}$N and $^{13}$N excitation-energy spectra deduced with the invariant-mass method for detected $p+^{11}$C and $p+^{12}$C events, respectively. These spectra were measured simultaneously with the $^{12}$O and $^{12}$N two-proton decay data to be presented later. The first spectrum is dominated by a peak corresponding to the first-excited state of $^{12}$N [$E^* = 960(12)$ keV] which is produced very strongly in proton-knockout reactions. The peak in the second spectrum can be associated with a known $E^* = 3502(2)$ keV, $J^\pi = 3/2^-$ level in $^{13}$N [23].

The decay widths of the two states considered above are $\Gamma < 20$ keV and 62 keV, significantly less than the experimental values of 82 and 280 keV [23], respectively, and thus these widths are dominated by the experimental resolution. The solid curves in Figs. 2(a) and 2(b) show the results of simulations using intrinsic Beit-Wigner line shapes with the experimental resolution incorporated via Monte Carlo simulations taking into account the detector's angular and energy resolutions. The excitation-energy resolution is largely insensitive to the beam quality (beam-spot size and momentum resolution) and the energy loss of the beam in the target, rather it is very sensitive to processes that cause changes in the detected relative velocities of the decay products. The largest contribution to the final resolution is associated with the target thickness including small-angle scattering [24] and the differential velocity loss of the protons and C fragments in leaving the target [25]. The initial simulations overestimated the widths of the peaks slightly (9%), and this was found to be associated with longitudinal decays which are more sensitive to the differential velocity loss. We subsequently reduced the differential velocity loss from the tabulated values in Ref. [25] to obtain the curves in Figs. 2(a) and 2(b). These simulations were then used to determine the experimental response for two-proton decay.

The peak centroids are well reproduced by these simulations. We subsequently allowed the centroids of the Bret-Wigner line shapes to vary and fit the spectra obtaining values of $E^* = 968$ keV ($^{12}$N) and 3496 keV ($^{13}$N) with 2 keV statistical errors. These are in excellent agreement with the tabulated values of 960(12) and 3502(2) keV [23] and thus we assign a systematic uncertainty of 10 keV to all our extracted excitation energies and mass excesses.

The reconstructed spectrum of total kinetic energy $E_T$ released in the decay of $^{12}$O is shown in Fig. 2(c) after a small background removal. Particle identification was obtained with the $\Delta E$-$E$ method, but complete separation of C isotopes was not achieved. The most important contributions to this problem are the channeling interactions in the Si $\Delta E$ detector, which result in 5% of $^{11}$C fragments leaking into the $^{10}$C gate. This fraction was determined from nominal $p+^{10}$C events where the excitation-energy spectrum showed a peak associated with the very strong $p+^{11}$C channel of Fig. 2(a). For the $2p+^{10}$C events, there is contamination from two previously unknown levels in $^{13}$O (created via inelastic excitation of the projectile) which undergo sequential two-proton decay with $E_T = 0.9$ and 1.6 MeV. The latter is more intense and also has the same $E_T$ value as $^{12}$O$_{g.s.}$ decay, thus these events also will populate the prominent $^{12}$O ground-state peak visible in Fig. 2(c) at $E_T = 1.64$ MeV. However, this background is easily determined by analyzing detected $2p+^{11}$C events as if the carbon fragments have $A = 10$. The resulting background spectrum has a broader peak (FWHM $\sim$ 500 keV) at $E_T = 1.6$ due to incorrect mass assignment, and subtraction of this spectrum reduces the height of the ground-state peak by only $\sim$15%. The contribution of channeling to the backgrounds of the other spectra presented in the work was found be minimal.

The background-subtracted $^{12}$O ground-state peak has an experimental width of only $\sim$230 keV already inconsistent with 578(205) keV value measured by Kryger *et al.* [1]. The peak centroid of $E_T = 1.638(24)$ MeV is also 134 keV smaller than the value expected based on the tabulated $^{12}$O$_{g.s.}$ mass [2] which is listed with an uncertainty of 18 keV. A broad excited state is also observed at $E_T = 3.606$ MeV ($E^* = 1.968$ MeV). This might be same state observed by Suzuki *et al.* [13], although Sherr and Fortune suggest that both a $2^+$ and a $0^+$ state are expected near this energy [26]. Clearly the statistical uncertainties are not sufficient to determine whether this structure is a singlet or doublet. In the subsequent analysis we have assumed it to be a singlet.

The solid curve in Fig. 2(c) shows a $\chi^2$ fit to the spectrum assuming Bret-Wigner line shapes for the ground- and excited-state peaks and including the experimental resolution using the Monte Carlo simulations. The width of the ground-state peak was found to be consistent with the experimental resolution. The fitted width is $\Gamma = 10(34)$ keV with an upper limit of 72 keV at the $3\sigma$ level. This result is inconsistent with all the previously published experimental values but in line with the theoretical estimates. The mass excess for the two levels, obtained by adding the mass excesses of the decay products to $E_T$, are listed in Table I along with centroids and widths obtained from the $\chi^2$ fits.

The $^{12}$N $E_T$ spectrum from $2p+^{10}$B events, shown in Fig. 2(d), displays a peak at 1.165 MeV corresponding to an excitation energy of 10.45 MeV if $^{10}$B was formed in its ground state. In principle, the detected $^{10}$B fragment could have also been formed in more than four excited states which $\gamma$ decay [27,28], and thus its excitation energy may be larger than 10.45 MeV. The two-proton decay of the isobaric analog state is expected to populate the 1.740 MeV $^{10}$B state which subsequently decays by $\gamma$-ray emission [27] [Fig. 1(b)]. If the observed peak is the IAS, then the level energy would be 12.19 MeV, exactly at the energy expected by the IMME (see later). A $\chi^2$ fit to this peak with an exponential background

TABLE I. For the two-proton-decay states measured in this work, this table lists the total kinetic energy released in the decay ($E_T$), the excitation energy ($E^*$), the mass excess ($\Delta M$), the decay width ($\Gamma$), and the spin and parity of the level.

| Nucl. | $E_T$ (MeV) | $E^*$ (MeV) | $\Delta M$ (MeV) | $\Gamma$ (keV) | $J^\pi$ |
|---|---|---|---|---|---|
| $^{12}$O | 1.638(24) | 0 | 31.914(24) | <72 | $0^+$ |
| $^{12}$O | 3.606(60) | 1.968(52) | 33.882(60) | 475(110) | |
| $^{12}$N | 1.165(29) | 12.196(29) | 29.534(29) | < 110 | $0^+$ |
| $^{12}$N | ~3.17 | ~14.20 | ~31.54 | | |

TABLE II. Mass excesses for the $A = 12$ isospin $T = 2$ quintet and the coefficients obtained from quadric, cubic, and quartic fits with $\chi^2$ per degree of freedom.

| Nucl. | $T_Z$ | Mass excess (keV) | Ref. | $a, b, c$ (keV) | $a, b, c, d$ (keV) | $a, b, c, d, e$ (keV) |
|---|---|---|---|---|---|---|
| Be | 2 | 25.0780 (21) | [31] | $a = 27596$ (2) | $a = 27596$ (2) | $a = 27596$ (2) |
| B | 1 | 26.111 (15) | [30] | $b = -1709$ (6) | $b = -1711$ (18) | $b = -1712$ (22) |
| C | 0 | 27.5950 (24) | [2,23] | $c = 225$ (3) | $c = 225$ (3) | $c = 227$ (22) |
| N | −1 | 29.534 (29) | This work | $\chi^2/n = 0.011$ | $d = 0.5$ (47) | $d = 0.8$ (58) |
| O | −2 | 31.914 (24) | This Work | | $\chi^2/n = 0.008$ | $e = -0.5$ (56) |

is shown by the solid curve in Fig. 2(d). The peak width is again consistent with the experiment resolution with a limit of $\Gamma < 110$ keV at the $3\sigma$ level. No such narrow $^{12}$N levels are known above $E^* = 10$ MeV and its seems highly likely from this fact alone that this is the isobaric analog state.

There is evidence of another possibly wide peak at $E_T \sim 3.17$ MeV as shown by the fitted curve in Fig. 2(d). However, the fit was not well constrained due to the relatively large background and statistical errors. Fitted peak characteristics depend very much on the assumed $E_T$ dependence of the background. The energy separation between this peak and the IAS peak is very similar to that between the two peaks in Fig. 2(c) suggesting this second peak is the analog of the excited $^{12}$O state and thus $T = 2$. As such it would be expected to sequentially two-proton decay to the IAS in $^{10}$B through either the $1/2^+$ or the $1/2^-$, $T = 3/2$ levels in $^{11}$C [29] conserving isospin.

With the detection of the IAS in $^{12}$N, the $T = 2$ isobaric quintet for $A = 12$ is complete. The mass excesses for the quintet are listed in Table II. For $^{12}$B, we have used a value obtained from the invariant mass of $\alpha$+$^8$Li decays of the parent $^{12}$B fragment formed in $^{12}$Be$(p,n)^{12}$B$_{\rm IAS}$ reactions with high statistical accuracy [30]. As in this work, "calibration" peaks were found to ascertain the systematic error which dominates the final uncertainty.

The results of a quadratic, cubic, and quartic fits to the IMME are summarized in Table II and the residuals from the quadratic fit are plotted in Fig. 3. These residuals are all consistent with zero and thus the mass excesses are clearly consistent with the quadratic form of the IMME expected for isospin symmetry. The $d$ coefficient for the cubic fit is 0.5(47) keV which is consistent with zero. This can be compared to values of 47(22), 11.1(23), and 6.3(16) keV in the $A = 7, 8$, and 9 multiplets, respectively, where large deviations from the quadratic fit are known [20].

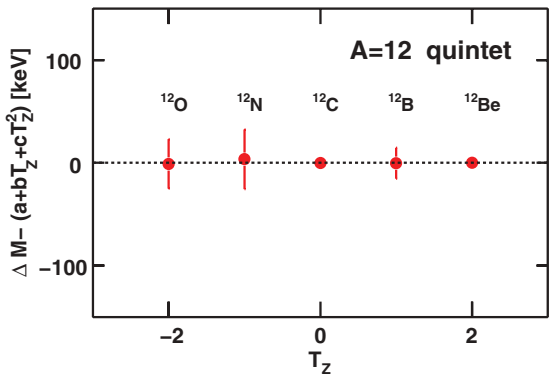


FIG. 3. (Color online) Deviations from the fitted quadratic form of the IMME for the $A = 12$ quintet.

Although the IMME fits the data quite well, this does not rule out all aspects of isospin asymmetries. For multiplets where the proton-rich members are at or near the continuum, the wave functions of the last proton extend farther out compared to the analog neutrons in the bound neutron-rich members. This effect is enhanced for nucleons in $s$ orbits where the effect is called the Thomas-Ehrman shift. These isospin asymmetries are mostly absorbed into the $b$ and $c$ coefficients of the IMME and produce very small $d$ values [18,32]. Grigorenko *et al.* [17] predict that a three-body-body Thomas-Ehrman effect breaks the isospin symmetry between $^{12}$O$_{\rm g.s.}$ and its mirror $^{12}$Be$_{\rm g.s.}$ to the level of some tens of percent with $^{12}$O having more $s^2$ content. It is quite possible this effect is also absorbed into the $b$ and $c$ coefficients and not visible from our present analysis.

If we approximate the nucleus as a homogeneous sphere of radius $R$, then the last two coefficients of the IMME are [18,32]

$$b = -0.6\frac{(A-1)e^2}{R} + (M_n - M_{^1H}), \tag{2}$$

$$c = \frac{0.6e^2}{R}. \tag{3}$$

Refitting the data with just two fitting parameters, $a$ and $R$, one obtains essentially the same fit as before and the fitted equivalent-sharp-sphere radius is $R = 3.809(3)$ fm. This can be compared to values of $R = 3.435(1)$ fm ($J^\pi = 1^+$) and $R = 3.370$ (2) fm ($J^\pi = 2^+$) obtained from fitting the two lowest energy $T = 1$ triplets for $A = 12$. The quintet has a larger radius than the triplets and this probably reflects the expanded size of the quintet systems due to their lower separation energies and the three-body Thomas-Ehrman effect which lowers the Coulomb energy in the proton-rich systems.

In summary we have created $^{12}$O fragments via neutron knockout from a $^{13}$O projectile. The three decay products produced in the two-proton decay of the ground and an excited state were detected and the $^{12}$O mass and width were determined with the invariant mass method. The width of the ground state was found to be less than 72 keV, inconsistent with previous published experimental results but consistent with theoretical estimates. The isobaric analog state of $^{12}$O$_{\rm g.s.}$

in $^{12}$N was observed for the first time, produced via proton knockout reactions from the $^{13}$O beam. While single-nucleon decay of this state cannot conserve both energy and isospin, two-proton decay to the isobaric analog in $^{10}$B does. Thus to the extent that isospin is conserved, this represents a Goldansky-type two-proton decay of the type previously seen for the isobaric analog of $^{8}$C in $^{8}$B [11]. With the new mass excesses measured for $^{12}$O and its analog state, we have found that the $A = 12$ quintet can be fitted with the parabolic form of the isobaric multiplet mass equation which is required for isospin symmetry and not consistent with the magnitude of the deviations measured previously for the $A = 7$ and 9 quartets and the $A = 8$ quintet.

This work was supported by the US Department of Energy, Division of Nuclear Physics under Grants No. DE-FG02-87ER-40316, No. DE-FG02-93ER40773, and No. DE-SC004972.

[1] R. A. Kryger, A. Azhari, M. Hellström, J. H. Kelley, T. Kubo *et al.*, Phys. Rev. Lett. **74**, 860 (1995).
[2] G. Audi and W. Meng (private communication).
[3] A. Azhari, R. A. Kryger, and M. Thoennessen, Phys. Rev. C **58**, 2568 (1998).
[4] V. I. Goldansky, Nucl. Phys. **19**, 482 (1960).
[5] L. Axelsson, M. J. G. Borge, S. Fayans, V. Z. Goldberg, S. Grévy *et al.*, Phys. Rev. C **54**, R1511 (1996).
[6] K. Markenroth, L. Axelsson, S. Baxter, M. J. G. Borge, C. Donzaud *et al.*, Phys. Rev. C **62**, 034308 (2000).
[7] J. M. Oliveira, A. Lépine-Szily, H. G. Bohlen, A. N. Ostrowski *et al.*, Phys. Rev. Lett. **84**, 4056 (2000).
[8] V. Guimarães, S. Kubono, F. C. Barker, M. Hosaka, S. C. Jeong *et al.*, Phys. Rev. C **67**, 064601 (2003).
[9] E. Casarejos, C. Angulo, P. J. Woods, F. C. Barker, P. Descouvemont *et al.*, Phys. Rev. C **73**, 014319 (2006).
[10] L. V. Grigorenko, T. D. Wiser, K. Mercurio, R. J. Charity, R. Shane *et al.*, Phys. Rev. C **80**, 034602 (2009).
[11] R. J. Charity, J. M. Elson, J. Manfredi, R. Shane, L. G. Sobotka *et al.*, Phys. Rev. C **84**, 014320 (2011).
[12] G. J. KeKelis, M. S. Zisman, D. K. Scott, R. Jahn, D. J. Vieira *et al.*, Phys. Rev. C **17**, 1929 (1978).
[13] D. Suzuki, H. Iwasaki, D. Beaumel, L. Nalpas, E. Pollacco *et al.*, Phys. Rev. Lett. **103**, 152503 (2009).
[14] H. T. Fortune and R. Sherr, Phys. Rev. C **68**, 034309 (2003).
[15] R. Ivie, Master's thesis, University of Pennsylvania, 1992.
[16] F. C. Barker, Phys. Rev. C **59**, 535 (1999).
[17] L. V. Grigorenko, I. G. Mukha, I. J. Thompson, and M. V. Zhukov, Phys. Rev. Lett. **88**, 042502 (2002).
[18] W. Benenson and E. Kashy, Rev. Mod. Phys. **51**, 527 (1979).
[19] J. Britz, A. Pape, and M. S. Antony, At. Data Nucl. Data Tables **69**, 125 (1998).
[20] R. J. Charity, J. M. Elson, J. Manfredi, R. Shane, L. G. Sobotka *et al.*, Phys. Rev. C **84**, 051308 (2011).
[21] R. E. Tribble, R. H. Burch, and C. A. Gagliardi, Nucl. Instrum. Methods A **285**, 411 (1989).
[22] R. E. Tribble, C. A. Gagliardi, and W. Liu, Nucl. Instrum. Methods B **56/57**, 956 (1991).
[23] Evaluated Nuclear Structure Data File (ENSDF), http://www.nndc.bnl.gov/ensdf/ .
[24] R. Anne, J. Herault, R. Bimbot, H. Gauvin, C. Bastin, and F. Hubert, Nucl. Instrum. Methods B **34**, 295 (1988).
[25] J. F. Ziegler, J. P. Biersack, and U. Littmark, The Stopping and Range of Ions in Solids (Pergamon, New York, 1985), the code SRIM can be found at www.srim.org.
[26] H. T. Fortune and R. Sherr, Phys. Rev. C **82**, 034325 (2010).
[27] Y. S. Park, A. Niiler, and R. A. Lindgren, Phys. Rev. C **8**, 1557 (1973).
[28] J. Keinonen and A. Anttila, Nucl. Phys. A **330**, 397 (1979).
[29] B. Watson, C. Chang, and M. Hasinoff, Nucl. Phys. A **173**, 634 (1971).
[30] R. J. Charity, S. A. Komarov, L. G. Sobotka, J. Clifford, D. Bazin *et al.*, Phys. Rev. C **78**, 054307 (2008).
[31] S. Ettenauer, M. Brodeur, T. Brunner, A. T. Gallant, A. Lapierre *et al.*, Phys. Rev. C **81**, 024314 (2010).
[32] J. Jänecke, in *Isospin in Nuclear Physics*, edited by D. H. Wilkinson (North-Holland, Amsterdam, 1969), p. 299.